MECHANICAL BEHAVIOR OF FUNCTIONALLY GRADED NANO-CYLINDERS UNDER RADIAL PRESSURE BASED ON STRAIN GRADIENT THEORY

M. Shishesaz **M. Hosseini***

Department of Mechanical Engineering
Shahid Chamran University of Ahvaz
Ahvaz, Iran

ABSTRACT

In this paper, the mechanical behavior of a functionally graded nano-cylinder under a radial pressure is investigated. Strain gradient theory is used to include the small scale effects in this analysis. The variations in material properties along the thickness direction are included based on three different models. Due to slight variations in engineering materials, the Poisson's ratio is assumed to be constant. The governing equation and its corresponding boundary conditions are obtained using Hamilton's principle. Due to the complexity of the governed system of differential equations, numerical methods are employed to achieve a solution. The analysis is general and can be reduced to classical elasticity if the material length scale parameters are taken to be zero. The effect of material index n, variations in material properties and the applied internal and external pressures on the total and high-order stresses, are well examined. For the cases in which the applied external pressure at the inside (or outside) radius is zero, due to small effects in nano-cylinder, some components of the high-order radial stresses do not vanish at the boundaries. Based on the results, the material inhomogeneity index n, as well as the selected model through which the mechanical properties may vary along the thickness, have significant effects on the radial and circumferential stresses.

Keywords: Nano-cylinder, Strain gradient theory, Stress analysis, Functionally graded materials (FGMs), Size effect.

1. INTRODUCTION

During the past several years, some specific nano-structures, such as nanopillars, nanocones, nanofilaments, re-entrant surface curvatures and nano-cylinders have been fabricated. These nano-structures have characteristics suitable for various applications in nano-antenna, plasmonic antenna [1], plasmonic sensors [2], lasers [3, 4], broadband nonclassical light emission [5] and nanomedicines [6]. Also, Nano-cylinders are used extensively in the field of medical science as drug delivery vehicles as well as in mechanics. Even though anisotropic materials with nanometer-scale dimensions have been extensively explored in a diversified range of research areas, mechanical behavior of nano-cylinders has not been studied specifically. Therefore mechanical behavior of these structures becomes essential for their optimum use in human bodies. Due to inherent nano- size of these structures, classical elasticity theory is not capable of predicting their structural behavior, and hence, one of the non-classical theories, such as nonlocal elasticity theory [7-11], strain gradient theory [12-15], surface stress theory [16] or couple stress theory [17-19] should be used instead. These non-classical theories have the ability to include the size-effects in nano-structures. In addition to this, functionally graded materials (FGM) have large applications in various industries [20-26]. Material properties of FGM change gradually and continuously. On the nano-scale level, since material reactivity increases and chemical reactivity control becomes an important issue, then, functionally graded nano-cylinders become a good choice to control this behavior.

In recent years, many studies have been conducted in the field of nano-mechanics. Li and Hu [27] studied buckling behavior of a nonlinear Euler-Bernoulli simply supported beam based on nonlocal strain gradient theory. Hamilton's principle was used to drive the governing equation and the associated boundary conditions. Their results show that post-buckling deflection has a positive

* Corresponding author (s.m.hssini@gmail.com)

DOI : 10.1017/jmech.2018.10
Copyright © 2018 The Society of Theoretical and Applied Mechanics
https://doi.org/10.1017/jmech.2018.10 Published online by Cambridge University Press

relation with nonlocal parameters and an inverse relation with material characteristic parameter. Also, size dependent parameters showed a significant effect on the higher-order buckling deflection. Rezaeii-Pajand and Yaghoobi [28] offered a new formulation based on strain gradient theory for linear and geometric non-linear membrane elements. They used a new triangular element to formulate the problem. Li *et al*. [29] offered a model to investigate the flexural wave propagation in a functionally graded beam based on nonlocal strain gradient theory. The effect of some parameters such as nonlocal parameters and material characteristic parameters were investigated. Koochi *et al*. [30] investigated pull-in instability of beam type nano-electromechanical systems based on strain gradient theory. They showed the effects of electric fields and Casimir force on pull-in performance of nano-beams, based on strain gradient elasticity theory. Hosseini *et al*. [31] presented a complete stress analysis of a rotating functionally graded nanodisk with nonlinearly varying thickness, based on strain gradient theory. They showed that the nanodisk boundary conditions turn out to be different from those of a macro-disk. Shokrieh and Zibaei [32] derived the governing equations and their associated boundary conditions in nano-beams. Lazopoulos [33] studied the dynamic response of a thin elastic beam based on strain gradient theory. Variational method and simple linear strain gradient elastic theory along with surface energy was used to obtain the governing equation of motion and its associated boundary conditions. Their results showed that the new terms associated with the couple stresses have a significant effect on the stiffness of the thin beam. Ansari *et al*. [34] studied bending, buckling and free vibration of FG mindlin micro-plates. They employed modified strain gradient elasticity theory to explain the size effects on final results. Hamilton's principle was used to obtain the governing equation and its corresponding boundary conditions. Thai and Kim [35] analyzed bending and free vibration of functionally graded Reddy plate based on a modified couple stress theory. They found that small-scale effects become important when the plate thickness is small. Vatankhah and Kahrobaiyan [36] studied free vibration of size-dependent micro-resonators in the frameworks of strain gradient theory. They considered clamped-clamped boundary conditions for their micro-beam models. Using strain gradient theory, Wang *et al*. [37] investigated the mechanical and thermal buckling of a nanotube that was resting on an elastic foundation. They used Euler-Bernoulli and Timoshenko beam theory in their analysis. Their results showed that critical buckling load is dependent on the size effects and elastic stiffness of the foundation. Farahmand *et al*. [38] developed Navier solution for buckling behavior of functionally graded rectangular micro-plates. They employed Kirchhoff plate theory and principle of minimum potential energy to derive the governing equation. Their work shows the effects of material properties and size-effect parameters on the critical buckling load. Li and Hu [39] investigated the post-buckling behavior of a functionally graded nanobeam based on nonlocal stress and strain gradient effects. The results of this study show the dependence of stiffness-hardening/softening effects on scaling parameters. Mohammadi *et al*. [40] investigated the effect of temperature on the vibration behavior of orthotropic mono-layer graphene sheet surrounded by an elastic medium based on the nonlocal elasticity theory. Natural frequencies were obtained using Navier and Levy solutions and compared with those of other works. Also, the effect of small-scale parameters, temperature and foundation characteristic parameters on natural frequencies were studied. Li *et al*. [41] investigated free vibrational behavior of functionally graded size-dependent Timoshenko beams on the basis of nonlocal strain gradient theory. They used Hamilton's principle to drive the governing equation and its associated boundary conditions. Li and Hu [42] used nonlinear Euler-Bernoulli and Timoshenko beam models along with nonlocal strain gradient theory to study the bending behavior of through thickness functionally graded size-dependent beams. They showed the effect of small-scale parameter and material inhomogeneity parameters on bending deflection and vibrational frequencies of the size-dependent beams. Li *et al*. [43] investigated the bending, buckling and vibrational behaviors of through the length functionally graded Euler-Bernoulli size-dependent beams. They used nonlocal strain gradient theory along with Hamilton's principle to obtain the governing equation and its associated boundary conditions. They used generalized differential quadrature method to solve these equations. Their results show the effect of grading index and size-dependent parameter(s) on mechanical behavior of small scale beams. Kananipour [44] presented static analysis of a rectangular nano-plate located on the elastic foundation, using nonlocal elasticity theory along with Kirchhoff and mindlin plate theories. He solved the governing equation using differential quadrature method. His results show the effects of Winkler foundation modulus, plate aspect ratios, and influence of small-scale coefficients on static behavior of the nano-plate based on different boundary conditions. Other researchers have also done valuable researches in the field of nano-mechanics [45-58].

The literature survey shows the lack of information on nano-cylinder behavior under different loading conditions (such as internal or external pressure). Due to the importance of such behavior, this paper thoroughly investigates the effects of physical models and size coefficients on mechanical behavior, as well as stress distribution in such cylinders subjected to an internal and/or external pressure(s). Three models will be used to

https://doi.org/10.1017/jmech.2018.10 Published online by Cambridge University Press

investigate the effect of material parameters on the resulting stress distribution. Strain gradient theory will be used to derive the governing equilibrium equations.

2. THEORY AND FORMULATION

In this section, the governing equations for a nano-cylinder are formulated based on strain gradient theory. In classical elasticity theory, strain energy density function, U, is dependent on the infinitesimal strain tensor, which is the symmetric part of the gradient of displacement field u. Instead, in strain gradient elasticity theory, second gradient of the displacement field u appears both in equations of motion and boundary conditions. The strain gradient elasticity theory introduces dilatation gradient tensor and the deviatoric stretch gradient tensor, as well as the symmetric rotation gradient. Strain tensor ε and gradient of strain tensor ξ are given as;

$$\varepsilon = \frac{1}{2}\left[\nabla u + (\nabla u)^T\right]$$
$$\xi = \nabla\varepsilon = \frac{1}{2}\nabla\left[\nabla u + (\nabla u)^T\right] \tag{1}$$

where u is radial displacement. The gradient in cylindrical coordinate is defined as;

$$\nabla \equiv e_r\frac{\partial}{\partial r} + e_\theta\frac{1}{r}\frac{\partial}{\partial\theta} + e_z\frac{\partial}{\partial z} \tag{2}$$

The radial and circumferential strains are:

$$\varepsilon = \begin{bmatrix} \frac{\partial u}{\partial r} & 0 & 0 \\ 0 & \frac{u}{r} & 0 \\ 0 & 0 & 0 \end{bmatrix}, \quad \varepsilon_r = \frac{\partial u}{\partial r}, \quad \varepsilon_\theta = \frac{u}{r} \tag{3}$$

Additionally, non-zero components of the second gradient of the displacement field u are:

$$\xi_{rrr} = \frac{\partial^2 u}{\partial r^2}$$
$$\xi_{\theta\theta r} = \frac{1}{r}\frac{\partial u}{\partial r} - \frac{u}{r^2} = \frac{\partial\left(\frac{u}{r}\right)}{\partial r}$$
$$\xi_{r\theta\theta} = \frac{1}{r}\frac{\partial u}{\partial r} - \frac{u}{r^2} = \frac{\partial\left(\frac{u}{r}\right)}{\partial r}$$
$$\xi_{\theta r\theta} = \frac{1}{r}\frac{\partial u}{\partial r} - \frac{u}{r^2} = \frac{\partial\left(\frac{u}{r}\right)}{\partial r} \tag{4}$$

In strain gradient theory uniform strain within the element is defined by ε_{ij} and ξ_{ijk} is linearly varying of strain ε_{jk} in the x_i direction. The relationships between stresses and strains are determined using Hooke's Law. For the plane strain condition, one may write the radial (σ_r) and tangential (σ_θ) stresses as;

$$\sigma_r = \frac{E}{(1+\upsilon)(1-2\upsilon)}\left((1-\upsilon)\varepsilon_r + \upsilon\varepsilon_\theta\right)$$
$$\sigma_\theta = \frac{E}{(1+\upsilon)(1-2\upsilon)}\left((1-\upsilon)\varepsilon_\theta + \upsilon\varepsilon_r\right) \tag{5}$$

where Poisson's ratio υ, is assumed to be constant. In general, Hook's law may be written as follows [59]:

$$\sigma_r = A\frac{\partial u}{\partial r} + B\frac{u}{r}$$
$$\sigma_\theta = B\frac{\partial u}{\partial r} + A\frac{u}{r} \tag{6}$$

where;

$$A = \frac{E(1-\upsilon)}{(1+\upsilon)(1-2\upsilon)}$$
$$B = \frac{E\upsilon}{(1+\upsilon)(1-2\upsilon)} \tag{7}$$

According to this theory, high-order stress tensor τ is defined as:

$$\tau_{ijk} = \tau_{jik} = \frac{\partial U}{\partial\xi_{ijk}} = \frac{1}{2}a_1\left(\delta_{ij}\xi_{kpp} + 2\delta_{jk}\xi_{ppi} + \delta_{ik}\xi_{jpp}\right) + 2a_2\delta_{jk}\xi_{ipp} + a_3\left(\delta_{ij}\xi_{ppk} + \delta_{ik}\xi_{ppj}\right) + 2a_4\xi_{ijk} + a_5\left(\xi_{jki} + \xi_{kji}\right). \tag{8}$$

where a_i's and δ_{ij} are the higher-order length scale material parameters and Kronecker's delta, respectively. Stresses ($\sigma_{ij} = \partial U/\partial\varepsilon_{ij}$) and high-order stresses ($\tau_{ijk} = \partial U/\partial\xi_{ijk}$) are corresponding to ε_{ij} and ξ_{ijk}, respectively.

Expanding Eq. (8) while using Eq. (3), the high-order stress components are expressed as:

$$\tau_{rrr} = 2(a_1+a_2+a_3+a_4+a_5)\frac{\partial^2 u}{\partial r^2} + 2(a_1+a_2+a_3)\frac{1}{r}\frac{\partial u}{\partial r} - 2(a_1+a_2+a_3)\frac{1}{r^2}u$$
$$\tau_{\theta\theta r} = \left(\frac{1}{2}a_1+a_3\right)\frac{\partial^2 u}{\partial r^2} + \left(\frac{1}{2}a_1+a_3+2a_4+2a_5\right)\frac{1}{r}\frac{\partial u}{\partial r} - \left(\frac{1}{2}a_1+a_3+2a_4+2a_5\right)\frac{1}{r^2}u$$
$$\tau_{r\theta\theta} = (a_1+2a_2)\frac{\partial^2 u}{\partial r^2} + (a_1+2a_2+2a_4+2a_5)\frac{1}{r}\frac{\partial u}{\partial r} - (a_1+2a_2+2a_4+2a_5)\frac{1}{r^2}u$$
$$\tau_{\theta r\theta} = \left(\frac{1}{2}a_1+a_3\right)\frac{\partial^2 u}{\partial r^2} + \left(\frac{1}{2}a_1+a_3+2a_4+2a_5\right)\frac{1}{r}\frac{\partial u}{\partial r} - \left(\frac{1}{2}a_1+a_3+2a_4+2a_5\right)\frac{1}{r^2}u \tag{9}$$

https://doi.org/10.1017/jmech.2018.10 Published online by Cambridge University Press

The following simplifications are used in order to simplify the process of obtaining the governing differential equations.

$$k_1 = 2\left(a_1 + a_2 + a_3 + a_4 + a_5\right) \quad k_2 = 2\left(a_1 + a_2 + a_3\right) \quad k_3 = k_7 = 1/2\, a_1 + a_3$$
$$k_4 = k_8 = 1/2\, a_1 + a_3 + 2a_4 + 2a_5 \quad k_5 = \left(a_1 + 2a_2\right) \quad k_6 = \left(a_1 + 2a_2 + 2a_4 + 2a_5\right)$$
$$D_1 = \left(3a_1 + 4a_2 + 2a_3 + 2a_4 + 2a_5\right) \quad D_2 = D_4 = \left(a_1 + a_3 + a_5\right) \quad D_3 = \left(a_1 + 4a_2 + 2a_4\right) \tag{10}$$

Therefore, Eq. (9) may be rewritten as;

$$\begin{Bmatrix} \tau_{rrr} \\ \tau_{\theta\theta r} \\ \tau_{r\theta\theta} \end{Bmatrix} = \begin{bmatrix} k_1 & \frac{k_2}{r} & -\frac{k_2}{r^2} \\ k_3 & \frac{k_4}{r} & -\frac{k_4}{r^2} \\ k_5 & \frac{k_6}{r} & -\frac{k_6}{r^2} \end{bmatrix} \begin{Bmatrix} \frac{\partial^2 u}{\partial r^2} \\ \frac{\partial u}{\partial r} \\ u \end{Bmatrix}, \quad \tau_{\theta r\theta} = \tau_{\theta\theta r} \tag{11}$$

In order to obtain the governing differential equation and its associated boundary conditions, minimum energy principle is used as follows.

$$\int_{t_1}^{t_2} \left(\delta U - \delta K - \delta W\right) dt = 0 \tag{12}$$

where W, K and U are the work done by the external loads, kinetic energy and total strain energy, respectively.

Variation of total strain energy may be written in terms of high-order stress components as;

$$\begin{aligned} \delta U &= \int_V \left(\sigma : \delta\varepsilon + \tau \vdots \delta\xi\right) dV = \int_V \left(\sigma_{jk}\delta\varepsilon_{jk} + \tau_{ijk}\delta\xi_{ijk}\right) dV \\ &= \int_0^{2\pi}\int_0^{h}\int_{r_i}^{r_o} \left(\sigma_r\delta\varepsilon_r + \sigma_\theta\delta\varepsilon_\theta + \tau_{rrr}\delta\xi_{rrr} + \tau_{\theta\theta r}\delta\xi_{\theta\theta r} + \tau_{r\theta\theta}\delta\xi_{r\theta\theta} + \tau_{\theta r\theta}\delta\xi_{\theta r\theta}\right) r dr dz d\theta \\ &= 2\pi\int_{r_i}^{r_o} \left(\sigma_r\delta\varepsilon_r + \sigma_\theta\delta\varepsilon_\theta + \tau_{rrr}\delta\xi_{rrr} + \tau_{\theta\theta r}\delta\xi_{\theta\theta r} + \tau_{r\theta\theta}\delta\xi_{r\theta\theta} + \tau_{\theta r\theta}\delta\xi_{\theta r\theta}\right) rh dr \end{aligned} \tag{13}$$

Additionally, any variation in the work done by the external loads is expressed as:

$$\delta W = 2\pi rh\left(\hat{\sigma}_r\delta u + \hat{\sigma}_\theta\delta v + \hat{\tau}_{rrr}\delta\varepsilon_{rr} + \hat{\tau}_{r\theta r}\delta\varepsilon_{r\theta} + \hat{\tau}_{\theta rr}\delta\varepsilon_{\theta r} + \hat{\tau}_{\theta\theta r}\delta\varepsilon_{\theta\theta}\right) \tag{14}$$

Since v, $\varepsilon_{r\theta}$ and $\varepsilon_{\theta r}$ are zero, then Eq. (14) is rewritten as:

$$\delta W = 2\pi rh\left(\hat{\sigma}_r\delta u + \hat{\tau}_{rrr}\delta\varepsilon_{rr} + \hat{\tau}_{\theta\theta r}\delta\varepsilon_{\theta\theta}\right) = 2\pi rh\left(\hat{\sigma}_r\delta u + \hat{\tau}_{rrr}\frac{d\delta u}{dr} + \hat{\tau}_{\theta\theta r}\frac{\delta u}{r}\right) = 2\pi rh\left(\left(\hat{\sigma}_r + \frac{\hat{\tau}_{\theta\theta r}}{r}\right)\delta u + \hat{\tau}_{rrr}\frac{d\delta u}{dr}\right) \tag{15}$$

In Eq. (15), r_o and r_i are the outer and inner radii of the nano-cylinder, respectively.

Substituting Eqs. (13) and (15) in Eq. (12) while using of Eqs. (3) and (4), the governing equilibrium equation and its corresponding boundary conditions are obtained. Note that due to axisymmetric loading condition, the displacement field is only a function of cylinder radius r.

$$\int_{r_i}^{r_o}\left(r\tau_{rrr}\frac{\partial^2\delta u}{\partial r^2} + \left(r\sigma_r + \tau_{\theta\theta r} + \tau_{r\theta\theta} + \tau_{\theta r\theta}\right)\frac{d\delta u}{dr} + \left(\sigma_\theta - \frac{\left(\tau_{\theta\theta r} + \tau_{r\theta\theta} + \tau_{\theta r\theta}\right)}{r}\right)\delta u\right) dr - 2\pi r\left(\left(\hat{\sigma}_r + \frac{\hat{\tau}_{\theta\theta r}}{r}\right)\delta u + \hat{\tau}_{rrr}\frac{d\delta u}{dr}\right) = 0 \tag{16}$$

Integrating Eq. (16) by parts while applying the variational principal, one may expanded this equation in the following form.

$$\begin{aligned} &\int_{r_i}^{r_o}\left(\frac{d^2\left(r\tau_{rrr}\right)}{dr^2} - \frac{d\left(r\sigma_r + \tau_{\theta\theta r} + \tau_{r\theta\theta} + \tau_{\theta r\theta}\right)}{dr} + \left(\sigma_\theta - \frac{\left(\tau_{\theta\theta r} + \tau_{r\theta\theta} + \tau_{\theta r\theta}\right)}{r}\right)\right)\delta u dr + \left(r\tau_{rrr} - r\hat{\tau}_{rrr}\right)\frac{\partial\delta u}{\partial r}\Big|_{r_i}^{r_o} \\ &+\left(\left(r\sigma_r + \tau_{\theta\theta r} + \tau_{r\theta\theta} + \tau_{\theta r\theta}\right) - \frac{d\left(r\tau_{rrr}\right)}{dr} - r\left(\hat{\sigma}_r + \frac{\hat{\tau}_{\theta\theta r}}{r}\right)\right)\delta u\Big|_{r_i}^{r_o} = 0 \end{aligned} \tag{17}$$

https://doi.org/10.1017/jmech.2018.10 Published online by Cambridge University Press

Consequently, the equilibrium equation and its associated boundary conditions may be written explicitly as;

equlibrium Equation :

$$\frac{d^2\left(r\tau_{rrr}\right)}{dr^2}-\frac{d\left(r\sigma_r+\tau_{\theta\theta r}+\tau_{r\theta\theta}+\tau_{\theta r\theta}\right)}{dr}+\left(\sigma_\theta-\frac{\left(\tau_{\theta\theta r}+\tau_{r\theta\theta}+\tau_{\theta r\theta}\right)}{r}\right)=0$$

Boundary Condition :

$$r\tau_{rrr}-r\hat{\tau}_{rrr}=0\rightarrow\tau_{rrr}=\hat{\tau}_{rrr}\quad @r=r_1,r_2$$

$$\left(r\sigma_r+\tau_{\theta\theta r}+\tau_{r\theta\theta}+\tau_{r\theta r}\right)-\frac{d\left(r\tau_{rrr}\right)}{dr}-r\left(\hat{\sigma}_r+\frac{\hat{\tau}_{\theta\theta r}}{r}\right)=0\quad @r=r_1,r_2 \tag{18}$$

On using Eqs. (6), (9) and (10), the equilibrium equation given by the first of Eq. (18) may be written in terms of displacement component u as;

$$\begin{aligned}
&rk_1\frac{d^4u}{dr^4}+\left(2r\frac{dk_1}{dr}+\left(2k_1+k_2-k_3-k_5-k_7\right)\right)\frac{d^3u}{dr^3}\\
&\quad+\left(-Ar+r\frac{d^2k_1}{dr^2}+\frac{d\left(2k_1+2k_2-k_3-k_5-k_7\right)}{dr}-\frac{1}{r}\left(k_2+k_3+k_4+k_5+k_6+k_7+k_8\right)\right)\frac{d^2u}{dr^2}\\
&\quad+\left(-\left(+\frac{dA}{dr}r+A\right)+\frac{d^2k_2}{dr^2}-\frac{1}{r}\frac{d\left(2k_2+k_4+k_6+k_8\right)}{dr}+\frac{1}{r^2}\left(2k_2+k_4+k_6+k_8\right)\right)\frac{du}{dr}\\
&\quad+\left(-\frac{dB}{dr}+\frac{1}{r}A-\frac{1}{r}\frac{d^2k_2}{dr^2}+\frac{1}{r^2}\frac{d\left(2k_2+k_4+k_6+k_8\right)}{dr}-\frac{1}{r^3}\left(2k_2+k_4+k_6+k_8\right)\right)u=0
\end{aligned} \tag{19}$$

while the boundary conditions are expressed as;

$$k_1\frac{d^2u}{dr^2}+\frac{1}{r}k_2\frac{du}{dr}-\frac{1}{r^2}k_2u=\hat{\tau}_{rrr}\quad @r=r_i,r_o \tag{20}$$

and

$$\begin{aligned}
&-rk_1\frac{d^3u}{dr^3}-\left(r\frac{dk_1}{dr}+\left(k_1+k_2-k_3-k_5-k_7\right)\right)\frac{d^2u}{dr^2}+\left(Ar+\frac{1}{r}\left(k_2+k_4+k_6+k_8\right)-\frac{dk_2}{dr}\right)\frac{du}{dr}\\
&+\left(B-\frac{1}{r^2}\left(k_2+k_4+k_6+k_8\right)+\frac{1}{r}\frac{dk_2}{dr}\right)u=r\left(\hat{\sigma}_r+\frac{\hat{\tau}_{\theta\theta r}}{r}\right)\quad @r=r_i,r_o
\end{aligned} \tag{21}$$

Since in strain gradient theory, the size effects appear in the high order stress components τ_{ijk} , then one can simply interpret their presence as mean to include the size effects that lack in classical elasticity theory.

To simplify the solution, these equations are non- dimensionalized using the following non-dimensional parameters.

$$\begin{aligned}
&\bar{r}=\frac{r}{r_o},\qquad \bar{k}_j\left(\bar{r}\right)=\frac{k_j\left(r\right)}{E_or_o^2}\quad j=1,2,...,8\\
&\bar{u}\left(\bar{r}\right)=\frac{u\left(r\right)}{r_o},\quad \bar{a}_j\left(\bar{r}\right)=\frac{a_j\left(r\right)}{E_or_o^2}\quad j=1,2,...,5\\
&\bar{A}\left(\bar{r}\right)=\frac{A\left(r\right)}{E_or_o^n},\qquad \bar{B}\left(\bar{r}\right)=\frac{B\left(r\right)}{E_or_o^n}
\end{aligned} \tag{22}$$

Accordingly, the dimensionless boundary conditions are expressed as:

$$\bar{k}_1\frac{d^2\bar{u}\left(\bar{r}\right)}{d\bar{r}^2}+\frac{1}{\bar{r}}\bar{k}_2\frac{d\bar{u}\left(\bar{r}\right)}{d\bar{r}}-\frac{1}{\bar{r}^2}\bar{k}_2\bar{u}=\frac{\hat{\tau}_{rrr}}{r_oE_o}\quad @\bar{r}=\bar{r}_i,1 \tag{23}$$

and

$$\begin{aligned}
&-\bar{r}\bar{k}_1\frac{d^3\bar{u}}{d\bar{r}^3}-\left(\bar{r}\frac{d\bar{k}_1}{d\bar{r}}+\left(\bar{k}_1+\bar{k}_2-\bar{k}_3-\bar{k}_5-\bar{k}_7\right)\right)\frac{d^2\bar{u}}{d\bar{r}^2}+\left(\bar{A}\bar{r}+\frac{1}{\bar{r}}\left(\bar{k}_2+\bar{k}_4+\bar{k}_6+\bar{k}_8\right)-\frac{d\bar{k}_2}{d\bar{r}}\right)\frac{d\bar{u}}{d\bar{r}}\\
&\quad+\left(\bar{B}-\frac{1}{\bar{r}^2}\left(\bar{k}_2+\bar{k}_4+\bar{k}_6+\bar{k}_8\right)+\frac{1}{\bar{r}}\frac{d\bar{k}_2}{d\bar{r}}\right)\bar{u}=\frac{\bar{r}}{E_o}\left(\hat{\sigma}_r+\frac{\hat{\tau}_{\theta\theta r}}{r_o\bar{r}}\right)\quad @\bar{r}=\bar{r}_i,1
\end{aligned} \tag{24}$$

https://doi.org/10.1017/jmech.2018.10 Published online by Cambridge University Press

Finally, the non-dimensional equilibrium equation is expressed as:

$$\begin{aligned}
&\bar{r}\bar{k}_1\frac{d^4\bar{u}}{d\bar{r}^4}+\left(2\bar{r}\frac{d\bar{k}_1}{d\bar{r}}+\left(2\bar{k}_1+\bar{k}_2-\bar{k}_3-\bar{k}_5-\bar{k}_7\right)\right)\frac{d^3\bar{u}}{d\bar{r}^3}\\
&+\left(-\bar{A}\bar{r}+\bar{r}\frac{d^2\bar{k}_1}{dr^2}+\frac{d\left(2\bar{k}_1+2\bar{k}_2-\bar{k}_3-\bar{k}_5-\bar{k}_7\right)}{dr}-\frac{1}{\bar{r}}\left(\bar{k}_2+\bar{k}_3+\bar{k}_4+\bar{k}_5+\bar{k}_6+\bar{k}_7+\bar{k}_8\right)\right)\frac{d^2\bar{u}}{d\bar{r}^2}\\
&+\left(-\left(+\bar{r}\frac{d\bar{A}}{d\bar{r}}+\bar{A}\right)+\frac{d^2\bar{k}_2}{dr^2}-\frac{1}{\bar{r}}\frac{d\left(2\bar{k}_2+\bar{k}_4+\bar{k}_6+\bar{k}_8\right)}{dr}+\frac{1}{\bar{r}^2}\left(2\bar{k}_2+\bar{k}_4+\bar{k}_6+\bar{k}_8\right)\right)\frac{d\bar{u}}{d\bar{r}}\\
&+\left(-\frac{d\bar{B}}{d\bar{r}}+\frac{1}{\bar{r}}\bar{A}-\frac{1}{\bar{r}}\frac{d^2\bar{k}_2}{dr^2}+\frac{1}{\bar{r}^2}\frac{d\left(2\bar{k}_2+\bar{k}_4+\bar{k}_6+\bar{k}_8\right)}{dr}-\frac{1}{\bar{r}^3}\left(2\bar{k}_2+\bar{k}_4+\bar{k}_6+\bar{k}_8\right)\right)\bar{u}=0
\end{aligned}\tag{25}$$

Due to complexity of the governing equations and its associate boundary conditions, a numerical scheme, namely differential quadrature method (DQM), is adapted for their solution. It is important to note that in contrast to classical theory, the boundary conditions appear in terms of two equations, namely Eqs. (23) and (24), which must be satisfied at both radii.

3. RESULTS AND DISCUSSION

In this section, the radial displacement, as well as the radial and circumferential stresses are presented based on strain gradient theory for three different models. According to these models, the modulus of elasticity in nano-cylinder may vary in the radial direction as;

Model 1:

$$E\left(r\right)=E_o e^{\left(\frac{r-r_i}{r_o-r_i}\right)^n}\qquad r_i<r<r_o\tag{26}$$

Model 2:

$$E\left(r\right)=\left(E_o-E_i\right)\left(\frac{r-r_i}{r_o-r_i}\right)^n+E_i\qquad r_i<r<r_o\tag{27}$$

Moel 3:

$$E\left(r\right)=E_o r^n\qquad r_i<r<r_o\tag{28}$$

where E_i and E_o are the modulus of elasticity at the inner and outer radii and n is the grading index. Here, the Poisson's ratio is kept constant. It should be noted that Eq. 22 is used for model 3 and act in the same way for other functions. Figure 1 illustrates the variation in the non-dimensional modulus of elasticity along the nano-cylinder radius for the three foregoing models.

Obviously, if in equilibrium Eq. (25) the size coefficients a_i (i =1, 2, 3, 4, 5) are set equal to zero, then the classical elasticity solution which is applicable to any *regular FGM cylinder* under proper boundary conditions, may be achieved. Under such conditions, the boundary condition (23) vanishes and the equilibrium Eq. (25) and its associated boundary condition (24) reduce into:

$$\left(\bar{A}\bar{r}\right)\frac{d^2\bar{u}}{d\bar{r}^2}+\left(+\bar{r}\frac{d\bar{A}}{d\bar{r}}+\bar{A}\right)\frac{d\bar{u}}{d\bar{r}}+\left(\frac{d\bar{B}}{d\bar{r}}-\frac{1}{\bar{r}}\bar{A}\right)\bar{u}=0\tag{29}$$

and

$$\bar{A}\frac{d\bar{u}}{d\bar{r}}+\bar{B}\frac{\bar{u}}{\bar{r}}=\frac{1}{E_i}\left(\hat{\sigma}_r\right)\quad @\,\bar{r}=\bar{r}_i,1\tag{30}$$

Doing so, the following properties are selected for a *regular functionally graded cylinder*; results of which are obtained numerically and compared with those of Chen and Lin [60] for a *macro* cylinder.

$$\begin{aligned}
&E_i=E_{Al}=70GPa\qquad E_o=E_{Cer}=151GPa\\
&\rho_i=\rho_{Al}=2700\frac{kg}{m^3}\quad \rho_o=\rho_{Cer}=5700\frac{kg}{m^3}\\
&\upsilon=0.3
\end{aligned}\tag{31}$$

A comparison of the results which are based on the present method and those of classical elasticity [60] is shown in Fig. 2. According to this figure, excellent agreements are observed between the two methods provided that in equilibrium equations, derived based on strain gradient theory, all size coefficients a_i (i =1, 2, 3, 4, 5) are set equal to zero.

However, in a nano-cylinder, $\bar{a}_i\neq 0$. Consequently, one may expect totally different results from those in Fig. 2. To investigate this behavior, mechanical properties of the materials composing the FGM nano-cylinder, and their associated material coefficients $\bar{a}_i$, are selected according to Tables 1 and 2 respectively.

3.1 The Effect of Material Inhomogeneity Parameter

The generated numerical results which are presented in this section explain the behavior of functionally graded nano-cylinder under internal and/or external pressure. The material properties are selected such that they correspond to pure Aluminum and Nickel placed at the inner and outer radii, respectively.

Figure 3 shows the effect of material inhomogeneity parameter n on non-dimensional radial stress $\bar{\sigma}_r$ for the three models introduced before. According to this figure, based on an internal pressure of 5 MPa, all three models

https://doi.org/10.1017/jmech.2018.10 Published online by Cambridge University Press

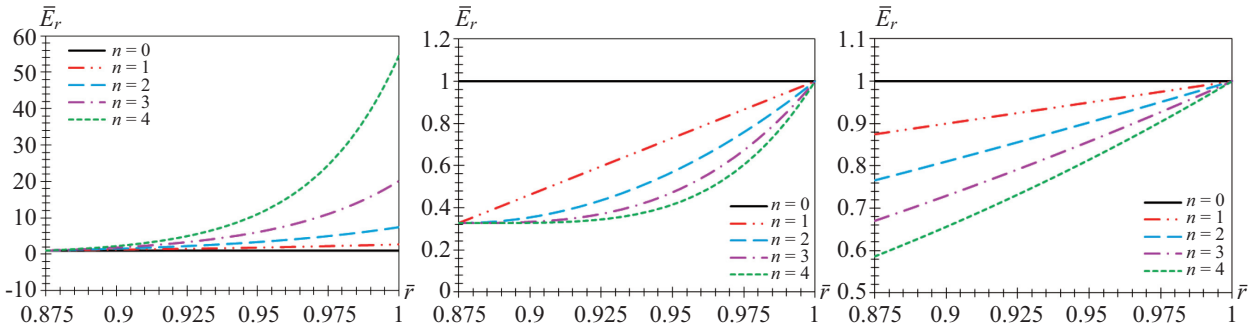


Fig. 1 Variations in the non-dimensional elastic modulus along the radius based on models 1, 2 and 3.

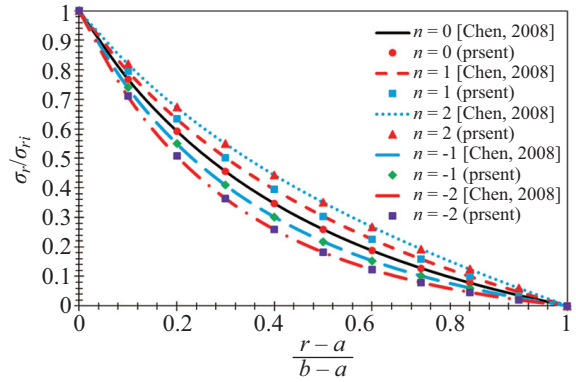


Fig. 2 Comparison of stresses in a regular FGM macro-cylinder based of classical elasity [60] and strain gradient theory with $a_i = 0$.

Table 1 Mechanical property of the selected materials

	material	E (GPa)	υ	α μm/(m-°C)	ρ (Kg/m^3)	K (W/(m-K))
1	Ni	207	0.31	13.1	8880	60.7
2	Al	68	0.36	25.5	2698.9	210

Table 2 Material constants a_i

	material	$\bar{a}_1$	$\bar{a}_2$	$\bar{a}_3$	$\bar{a}_4$	$\bar{a}_5$
1	Ni	0.2386	0.0134	0.0013	0.0934	0.2462
2	Al	0.1407	0.0027	-0.0083	0.0966	0.2584

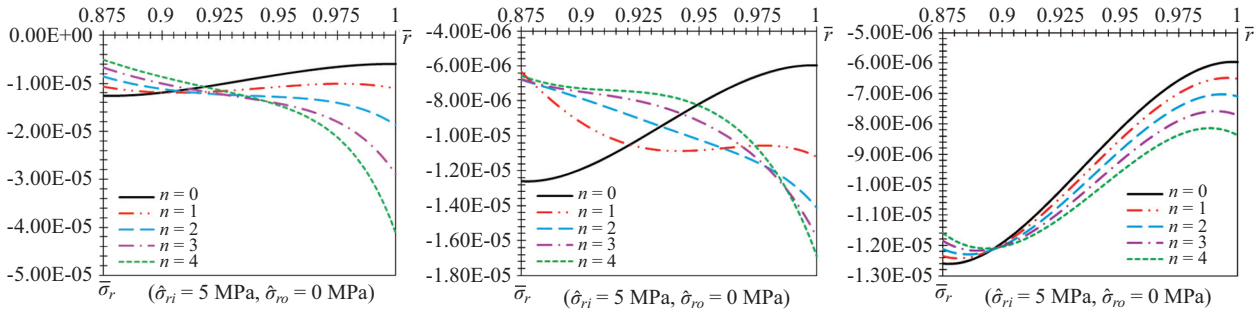
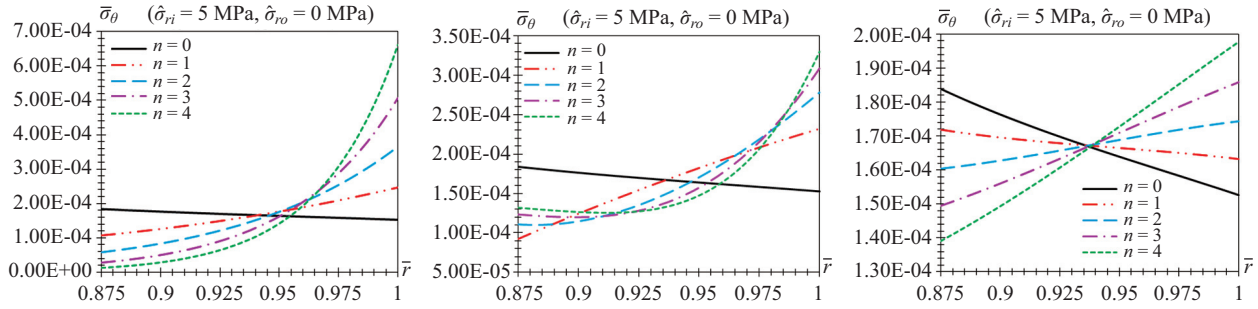


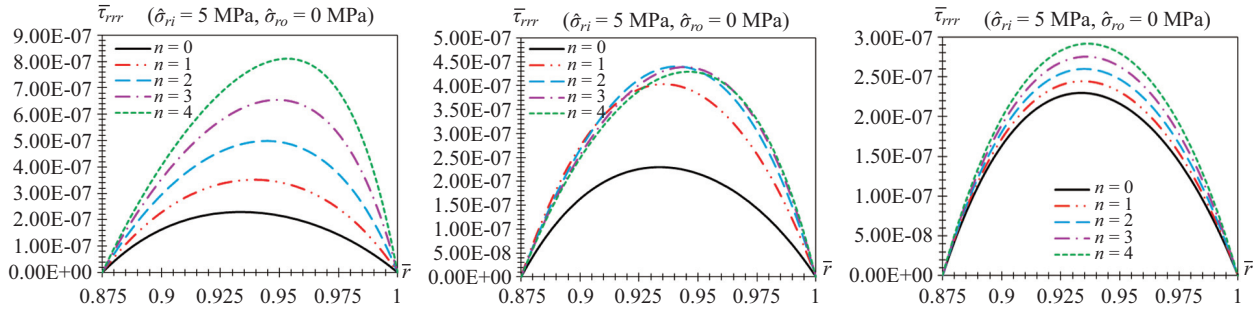
Fig. 3 The effect of material inhomogeneity index n on the non-dimensional radial stress in a nano-cylinder.

https://doi.org/10.1017/jmech.2018.10 Published online by Cambridge University Press



(a) Model 1 (b) Model 2 (c) Model 3

Fig. 4 The effect of material inhomogeneity index n on the non-dimensional circumferential stress in a nano-cylinder.



(a) Model 1 (b) Model 2 (c) Model 3

Fig. 5 The effect of material inhomogeneity index n on the non-dimensional high-order stress $\bar{\tau}_{rrr}$ in a nano-cylinder.

predict an increase in the absolute value of radial stress at the outside radius, as the gradient index n increases. However, in models 1 and 3, the opposite trend is observed at the inside radius.

On the other hand, model 3 shows a fluctuation in σ_r at the inside radius as n increases. In spite of zero external pressure at the outside radius, unlike classical theory, strain gradient theory predicts a non-zero value for $\bar{\sigma}_r$ at this location. This behavior is due to the application of strain gradient theory for nano-structures (in this case, a nano-cylinder) which cannot be predicted by the conventional classical elasticity.

Figure 4 shows the effect of material gradient inhomogeneity parameter n on the non-dimensional circumferential stress $\bar{\sigma}_\theta$. Similar behavior to that explained in Fig. 3 is observed for $\bar{\sigma}_\theta$ at both radii. However, in model 3, the values of circumferential stresses appear to have the same value at $\bar{r} = 0.898$.

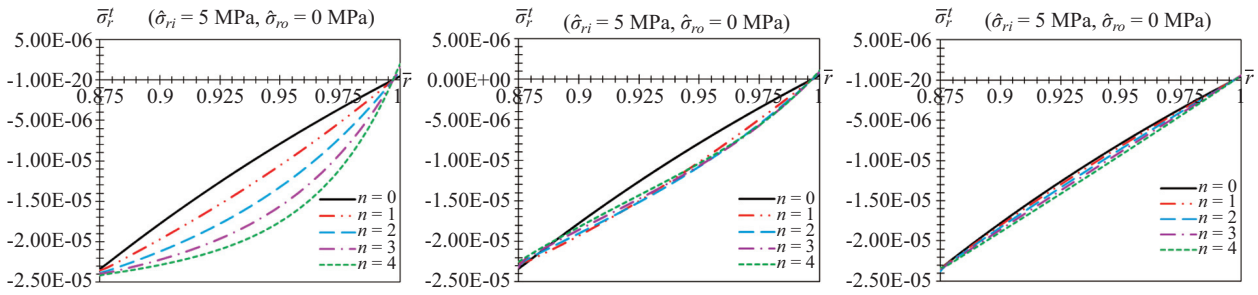
Distribution of non-dimensional high-order stress $\bar{\tau}_{rrr}$ versus the radial distance is shown in Figure 5. According to this figure, all three models predict zero $\bar{\tau}_{rrr}$ at both extreme radii. According to Eq. (18), $\bar{\tau}_{rrr}$ is one of the boundary conditions which has been assumed to be zero at the boundaries. Figures 5(a) and (b) indicate that models 1 and 3 predict a rise in this high-order stress component, as the gradient index n increases. According to model 2 (Fig. 5(b)), there appears to be a fluctuation in values of this stress component ($\bar{\tau}_{rrr}$) for any rise in n.

Figures 6 and 7 show the effect of n on the non-dimensional total radial and circumferential stresses, $\bar{\sigma}_r^t$ and $\bar{\sigma}_\theta^t$, respectively. Clearly, in spite of zero applied radial stress at the outside radius, strain gradient theory predicts non-zero stresses at this location. This observation is due to coupling effects between stresses and high-order stresses in nano-structures which are introduced in strain gradient theory. According to Fig. 6(c), in model 3, any change in material gradient index parameter n produces a small effect on non-dimensional radial stress in the nano-cylinder. Additionally, in this model, based on different values of n, the circumferential stresses have the same value at $\bar{r} = 0.933$. Moreover, in all three models, the non-dimensional circumferential stresses at the outside radius increase, as n increases. The inverse behavior is observed at the inner radius.

3.2 The Effect of Applied Pressure at the Inner and Outer Radii

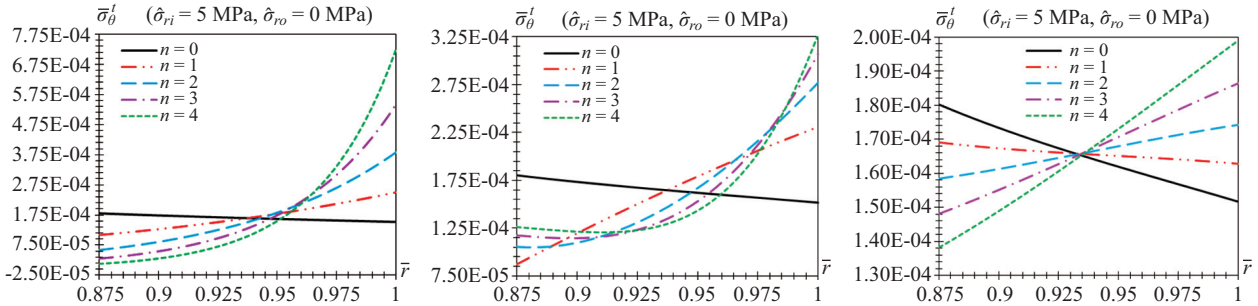
The effect of applied pressure at the inner and outer radii on the radial and circumferential stresses are shown in Figures 8 and 9, respectively. It is observed that for zero radial pressure either at the inside or outside radius, the resulting radial stress is nonzero at these two loca-

https://doi.org/10.1017/jmech.2018.10 Published online by Cambridge University Press



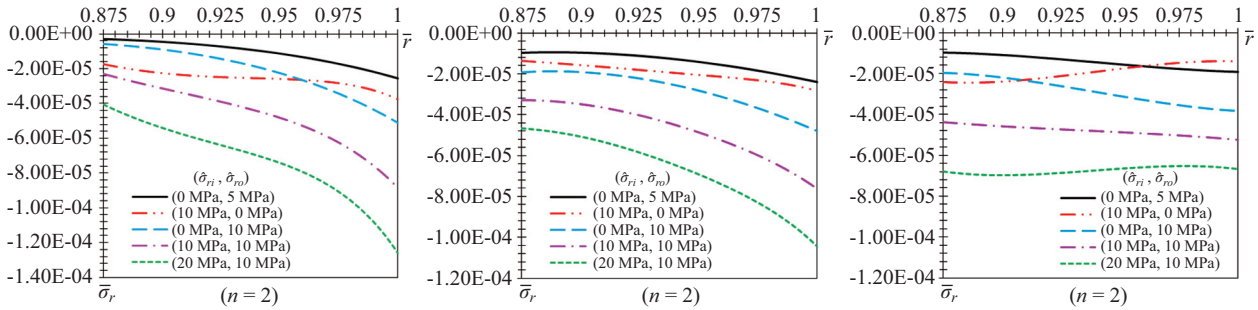
(a) Model 1 (b) Model 2 (c) Model 3

Fig. 6 The effect of material inhomogeneity index on the non-dimensional total radial stress of nano-cylinder.



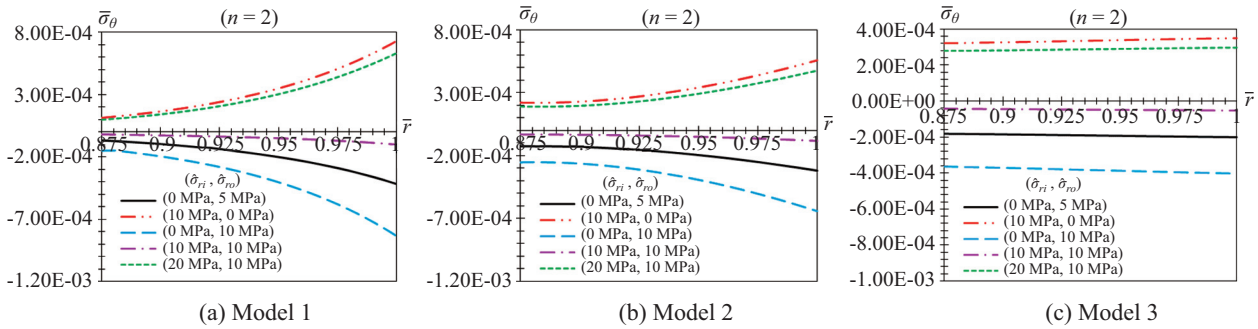
(a) Model 1 (b) Model 2 (c) Model 3

Fig. 7 The effect of material inhomogeneity index on the non-dimensional total circumferential stress of nano-cylinder.



(a) Model 1 (b) Model 2 (c) Model 3

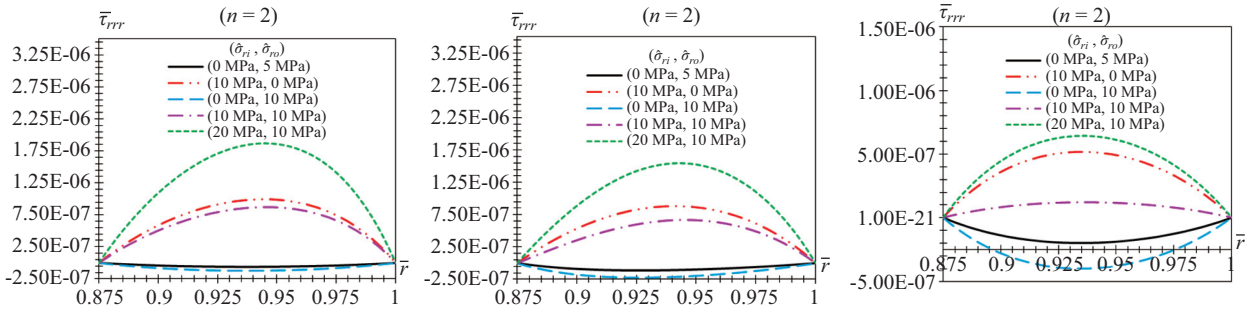
Fig. 8 The effect of applied pressure on the non-dimensional radial stress of nano-cylinder.



(a) Model 1 (b) Model 2 (c) Model 3

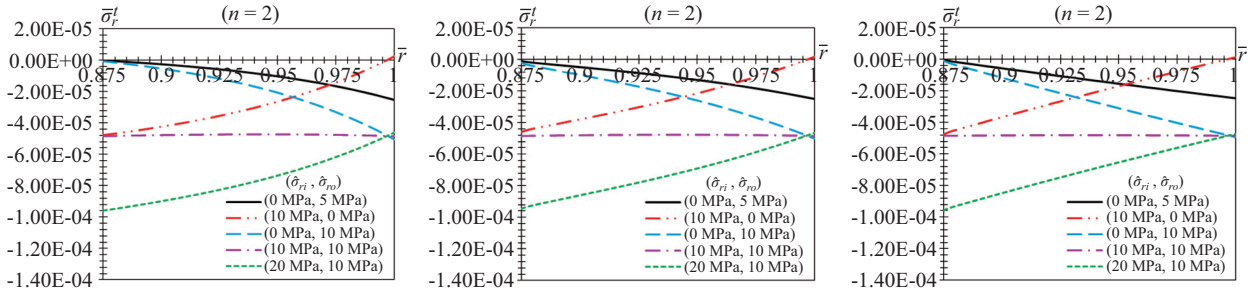
Fig. 9 The effect of applied pressure on the non-dimensional circumferential stress in a nano-cylinder.

https://doi.org/10.1017/jmech.2018.10 Published online by Cambridge University Press



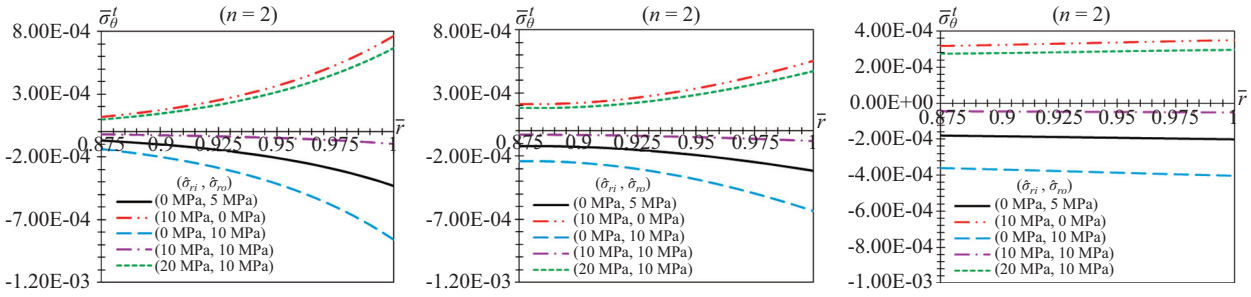
(a) Model 1 (b) Model 2 (c) Model 3

Fig. 10 The effect of applied pressure on the non-dimensional high-order stress $\bar{\tau}_{rrr}$ in a nano-cylinder.



(a) Model 1 (b) Model 2 (c) Model 3

Fig. 11 The effect of applied pressure on the non-dimensional total radial stress of nano-cylinder.



(a) Model 1 (b) Model 2 (c) Model 3

Fig. 12 The effect of applied pressure on non-dimensional total circumferential stress in nano-cylinder.

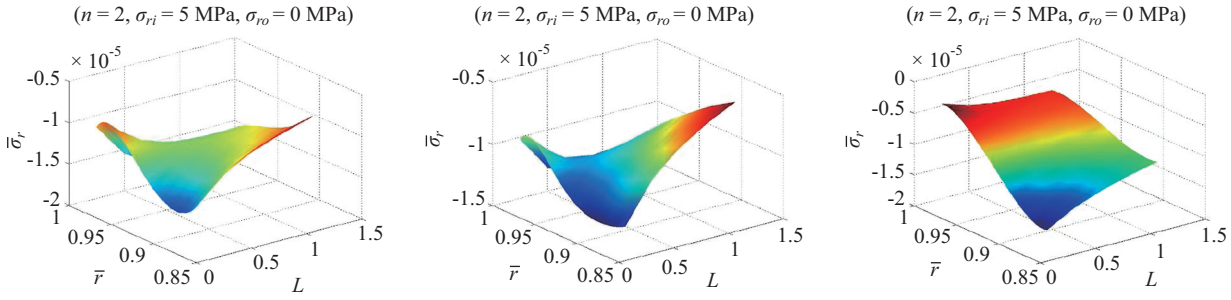
tions. For example, for the case in which $\hat{\sigma}_i = 10$ MPa and $\hat{\sigma}_o = 0$, the non-dimensional radial stress is nonzero at the outside radius. Any variations in the non-dimensional radial and circumferential stresses are strongly influenced by the material gradient index n and the type of model used in analysis (models 1, 2 and 3).

Figure 10 shows the effect of applied external pressure on the high-order stress $\bar{\tau}_{rrr}$. As mentioned before, unlike classical elasticity theory, the high-order stress $\bar{\tau}_{rrr}$ is one of the terms which appears in boundary conditions due to the application of strain gradient theory. Furthermore, it has been assumed that $\bar{\tau}_{rrr}$ is zero at the two boundaries (inner and outer radii). Application of the external pressure for a typical value of material index n = 2, seems to have a significant effect on this stress component.

According to Fig. 11, variation in total non-dimensional stress $\bar{\sigma}_r^t$ developed in nano-cylinder seems to be almost the same in all three models. The minute differences which exist between the results may be neglected. This result seems to be different for total tangential stress developed in nano-cylinder (see also Fig. 12 for $\bar{\sigma}_\theta^t$). According to Fig. 12(c), the (almost) linear distribution of total tangential stress seems to be quite different from those of the other two models.

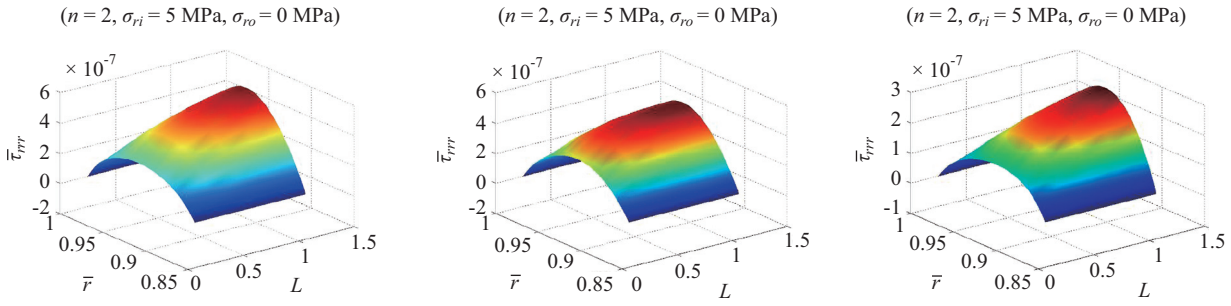
Assuming the length scale parameters given in Table 1

https://doi.org/10.1017/jmech.2018.10 Published online by Cambridge University Press



(a) Model 1 (b) Model 2 (c) Model 3

Fig. 13 The influence of small scale parameters on the non-dimensional radial stress.



(a) Model 1 (b) Model 2 (c) Model 3

Fig. 14 Influence of small scale parameters on $\bar{\tau}_{rrr}$.

are changed in the same proportion (using a scale parameter L) then, as shown in Eq. (32) one may write;

$$a_1 = 0.2386 \times L, \quad a_2 = 0.0134 \times L, \quad a_3 = 0.0013 \times L$$
$$a_4 = 0.0934 \times L, \quad a_5 = 0.2462 \times L \tag{32}$$

Figures 13 and 14 show the variations in the radial stress versus L at different locations in the radial direction for the models 1-3. Clearly, according to Fig. 13, the radial stress components $\bar{\sigma}_r$ show a complex variation in models 1 and 2. In model 3, the distribution seems to be simpler. In all three models, at the points closer to the outside radius, any increase in L, and hence the size factors a_i, results in an increase in the radial stress components.

According to Fig. 14, the variations in $\bar{\tau}_{rrr}$ seem to be almost the same in all three models for different values of L. Any change in L also seems to affect the values of $\bar{\tau}_{rrr}$.

4. CONCLUSIONS

In this article, the elastic solution of functionally graded nano-cylinder under internal and external pressures has been presented based on strain gradient theory. Three models were postulated in which the mechanical properties of nano-cylinder, except Poisson's ratio, were assumed to vary throughout the thickness. Comparison of the results based on strain gradient theory and those of others which were obtained for a regular macro-scale FGM cylinder proves the applicability of strain gradient for predicting stresses on macro-scale level, provided all size coefficients are set equal to zero. Additionally, in a nano-cylinder, even though the radial pressure at the inner or outer radii may be equal to zero, due to small scale effects, the non-zero radial high-order stress components occur at these two locations, a result that cannot be explained and predicted by the classical elasticity theory. Therefore, in nano-cylinders, classical elasticity theory is not well capable of predicting stresses, and hence, other theories, such a strain gradient theory, must be used instead. The numerical results which are based on three different models show that the small scale effects significantly contribute to a change in mechanical behavior of the nano-cylinder and the resulting stress distribution. These changes may not be neglected. Moreover, based on the results, material inhomogeneity index n, as well as the selected model through which the mechanical properties may vary along the thickness, have significant effects on the radial and circumferential stresses as well as high-order stress components in nano-cylinder.

REFERENCES

1. Aouani, H., Rahmani, M., Navarro-Cía, M. and Maier, S. A., "Third-Harmonic-Upconversion Enhancement from a Single Semiconductor Nanoparticle Coupled

https://doi.org/10.1017/jmech.2018.10 Published online by Cambridge University Press

to a Plasmonic antenna," *Nature Nanotechnology*, **9**, pp. 290-294 (2014).

2. Cai, G. *et al*., "Modeling and Design of a Plasmonic Sensor for High Sensing Performance and Clear Registration," *IEEE Photonics Journal*, **8**, pp. 1-11 (2016).
3. Nishikawa, T. *et al*., "Nanocylinder-Array Structure Greatly Increases the Soft X-Ray Intensity Generated from Femtosecond-Laser-Produced Plasma," *Applied Physics B*, **73**, pp. 185-188 (2001).
4. Karoro, A. *et al*., "Laser Nanostructured Co Nanocylinders-Al_2O_3 Cermets for Enhanced & Flexible Solar Selective Absorbers Applications," *Applied Surface Science*, **347**, pp. 679-684 (2015).
5. Maksymov, I. S. *et al*., "Metal-Coated Nanocylinder Cavity for Broadband Nonclassical Light Emission," *Physical Review Letters*, **105**, pp. 180502 (2010).
6. Salata, O., "Applications of Nanoparticles in Biology and Medicine," *Journal of Nanobiotechnology*, **2**, pp. 3 (2004).
7. Ebrahimi, F. and Barati, M. R., "Buckling Analysis of Smart Size-Dependent Higher Order Magneto-Electro-Thermo-Elastic Functionally Graded Nanosize Beams," *Journal of Mechanics*, **33**, pp. 23-33 (2016).
8. Mashat, D. S., Zenkour, A. M. and Sobhy, M., "Investigation of Vibration and Thermal Buckling of Nanobeams Embedded in An Elastic Medium under Various Boundary Conditions," *Journal of Mechanics*, **32**, pp. 277-287 (2015).
9. Wang, Y. G., Song, H. F. and Lin, W. H., "Nonlinear Pull-In Characterization of a Nonlocal Nanobeam with an Intermolecular Force," *Journal of Mechanics*, **32**, pp. 737-747 (2016).
10. Jandaghian, A. A. and Rahmani, O., "An Analytical Solution for Free Vibration of Piezoelectric Nanobeams Based on a Nonlocal Elasticity Theory," *Journal of Mechanics*, **32**, pp. 143-151 (2015).
11. Eringen, A. C., "Nonlocal Polar Elastic Continua," *International Journal of Engineering Science*,, **10**, pp. 1-16 (1972).
12. Ji, X., Li, A. Q. and Zhou, S. J., "The Strain Gradient Elasticity Theory in Orthogonal Curvilinear Coordinates and its Applications," *Journal of Mechanics*, pp. 1-13 (2016).
13. Shahriari, B. and Shirvani, S., "Small-Scale Effects on the Buckling of Skew Nanoplates Based on Non-Local Elasticity and Second-Order Strain Gradient Theory," *Journal of Mechanics*, pp. 1-10 (2017).
14. Aifantis, E. C., "Strain Gradient Interpretation of Size Effects," *International Journal of Fracture*, **95**, pp. 299-314 (1999).
15. Altan, B. and Aifantis, E., "On Some Aspects in the Special Theory of Gradient Elasticity," *Journal of the Mechanical Behavior of Materials (UK)*, **8**, pp. 231-282 (1997).
16. Zhou, S. S., Zhou, S. J., Li, A. Q. and Wang, B. L., "Analysis of Residual Stresses on the Vibration of a Circular Sensor Diaphragm with Surface Effects," *Journal of Mechanics*, **33**, pp. 323-329 (2016).
17. Keivani, M., Koochi, A. and Abadyan, M., "A New Bilayer Continuum Model Based on Gurtin-Murdoch and Consistent Couple-Stress Theories for Stability Analysis of Beam-Type Nanotweezers," *Journal of Mechanics*, **33**, pp. 137-146 (2016).
18. Ji, X. and Li, A. Q., "The Size-Dependent Electromechanical Coupling Response in Circular Micro-Plate Due to Flexoelectricity," *Journal of Mechanics*, pp. 1-11 (2016).
19. Ansari, R., Gholami, R. and Shahabodini, A., "Size-Dependent Geometrically Nonlinear Forced Vibration Analysis of Functionally Graded First-Order Shear Deformable Microplates," *Journal of Mechanics*, **32**, pp. 539-554 (2016).
20. Mazarei, Z., Nejad, M. and Hadi, A., "Thermo-Elasto-Plastic Analysis of Thick-Walled Spherical Pressure Vessels Made of Functionally Graded Materials," *International Journal of Applied Mechanics* (2016).
21. Ebrahimi, F., Ehyaei, J. and Babaei, R., "Thermal Buckling of FGM Nanoplates Subjected to Linear and Nonlinear Varying Loads on Pasternak Foundation," *Advances in Materials Research- An International Journal*, **5**, pp. 245-261 (2016).
22. Nejad, M., Rastgoo, A. and Hadi, A., "Exact Elasto-Plastic Analysis of Rotating Disks Made of Functionally Graded Materials," *International Journal of Engineering Science*, **85**, pp. 47-57 (2014).
23. Ebrahimi, F., "Dynamic Stability of FGM Cylindrical Shells," *Journal of Advanced Research in Mechanical Engineering*, **1** (2010).
24. Gharibi, M., Nejad, M. Z. and Hadi, A., "Elastic Analysis of Functionally Graded Rotating Thick Cylindrical Pressure Vessels with Exponentially-Varying Properties Using Power Series Method of Frobenius," *Journal of Computational Applied Mechanics*, **48**, pp. 89-98 (2017).
25. Ebrahimi, F. and Mokhtari, M., "Semi-Analytical Vibration Characteristics of Rotating Timoshenko Beams Made of Functionally Graded Materials," *Latin American Journal of Solids and Structures*, **12**, pp. 1319-1339 (2015).
26. Zamani Nejad, M., Jabbari, M. and Hadi, A., "A Review of Functionally Graded Thick Cylindrical and Conical Shells," *Journal of Computational Applied Mechanics*, **48**, pp. 357-370 (2017).
27. Li, L. and Hu, Y., "Buckling Analysis of Size-Dependent Nonlinear Beams Based on a Nonlocal Strain Gradient Theory," *International Journal of Engineering Science*, **97**, pp. 84-94 (2015).
28. Rezaiee-Pajand, M. and Yaghoobi, M., "An Efficient Formulation for Linear and Geometric Non-Linear Membrane Elements," *Latin American Journal of Solids and Structures*, **11**, pp. 1012-1035

https://doi.org/10.1017/jmech.2018.10 Published online by Cambridge University Press

(2014).

29. Li, L., Hu, Y. and Ling, L., "Flexural Wave Propagation in Small-Scaled Functionally Graded Beams via a Nonlocal Strain Gradient Theory," *Composite Structures*, **133**, pp. 1079-1092 (2015).
30. Koochi, A., Sedighi, H. M. and Abadyan, M., "Modeling the Size Dependent Pull-in Instability of Beam-Type NEMS Using Strain Gradient Theory," *Latin American Journal of Solids and Structures*, **11**, pp. 1806-1829 (2014).
31. Hosseini, M., Shishesaz, M., Tahan, K. N. and Hadi, A., "Stress Analysis of Rotating Nano-Disks of Variable Thickness Made of Functionally Graded Materials," *International Journal of Engineering Science*, **109**, pp. 29-53 (2016).
32. Shokrieh, M. M. and Zibaei, I., "Determination of the Appropriate Gradient Elasticity Theory for Bending Analysis of Nano-Beams by Considering Boundary Conditions Effect," *Latin American Journal of Solids and Structures*, **12**, pp. 2208-2230 (2015).
33. Lazopoulos, A., "Dynamic Response of Thin Strain Gradient Elastic Beams," *International Journal of Mechanical Sciences*, **58**, pp. 27-33 (2012).
34. Ansari, R. *et al*., "Size-Dependent Bending, Buckling and Free Vibration Analyses of Microscale Functionally Graded Mindlin Plates Based on the Strain Gradient Elasticity Theory," *Latin American Journal of Solids and Structures*, **13**, pp. 632-664 (2016).
35. Thai, H.-T. and Kim, S.-E., "A Size-Dependent Functionally Graded Reddy Plate Model Based on a Modified Couple Stress Theory," *Composites Part B: Engineering*, **45**, pp. 1636-1645 (2013).
36. Vatankhah, R. and Kahrobaiyan, M., "Investigation of Size-Dependency in Free-Vibration of Micro-Resonators Based on the Strain Gradient Theory," *Latin American Journal of Solids and Structures*, **13**, pp. 498-515 (2016).
37. Wang, B., Hoffman, M. and Yu, A., "Buckling Analysis of Embedded Nanotubes Using Gradient Continuum Theory," *Mechanics of Materials*, **45**, pp. 52-60 (2012).
38. Farahmand, H., Naseralavi, S. S., Iranmanesh, A. and Mohammadi, M., "Navier Solution for Buckling Analysis of Size-Dependent Functionally Graded Micro-Plates," *Latin American Journal of Solids and Structures*, **13**, pp. 3161-3173 (2016).
39. Li, L. and Hu, Y., "Post-Buckling Analysis of Functionally Graded Nanobeams Incorporating Nonlocal Stress and Microstructure-Dependent Strain Gradient Effects," *International Journal of Mechanical Sciences* (2016).
40. Mohammadi, M., Moradi, A., Ghayour, M. and Farajpour, A., "Exact Solution for Thermo-Mechanical Vibration of Orthotropic Mono-Layer Graphene Sheet Embedded in an Elastic Medium," *Latin American Journal of Solids and Structures*, **11**, pp. 437-458 (2014).
41. Li, L., Li, X. and Hu, Y., "Free Vibration Analysis of Nonlocal Strain Gradient Beams Made of Functionally Graded Material," *International Journal of Engineering Science*, **102**, pp. 77-92 (2016).
42. Li, L. and Hu, Y., "Nonlinear Bending and Free Vibration Analyses of Nonlocal Strain Gradient Beams Made of Functionally Graded Material," *International Journal of Engineering Science*, **107**, pp. 77-97 (2016).
43. Li, X., Li, L., Hu, Y., Ding, Z. and Deng, W., "Bending, Buckling and Vibration of Axially Functionally Graded Beams Based on Nonlocal Strain Gradient Theory," *Composite Structures*, **165**, pp. 250-265 (2017).
44. Kananipour, H., "Static Analysis of Nanoplates Based on the Nonlocal Kirchhoff and Mindlin Plate Theories Using DQM," *Latin American Journal of Solids and Structures*, **11**, pp. 1709-1720 (2014).
45. Akgöz, B. and Civalek, Ö., "Strain Gradient Elasticity and Modified Couple Stress Models for Buckling Analysis of Axially Loaded Micro-Scaled Beams," *International Journal of Engineering Science*, **49**, pp. 1268-1280 (2011).
46. Daneshmehr, A., Rajabpoor, A. and Hadi, A., "Size Dependent Free Vibration Analysis of Nanoplates Made of Functionally Graded Materials Based on Nonlocal Elasticity Theory with High Order Theories," *International Journal of Engineering Science*, **95**, pp. 23-35 (2015).
47. Nejad, M. Z. and Hadi, A., "Non-Local Analysis of Free Vibration of Bi-Directional Functionally Graded Euler–Bernoulli Nano-Beams," *International Journal of Engineering Science*, **105**, pp. 1-11 (2016).
48. Romanoff, J., Reddy, J. N. and Jelovica, J., "Using Non-Local Timoshenko Beam Theories for Prediction of Micro- and Macro-Structural Responses," *Composite Structures*, **156**, pp. 410-420 (2016).
49. Nejad, M. Z. and Hadi, A., "Eringen's Non-Local Elasticity Theory for Bending Analysis of Bi-Directional Functionally Graded Euler–Bernoulli Nano-Beams," *International Journal of Engineering Science*, **106**, pp. 1-9 (2016).
50. Akgöz, B. and Civalek, Ö., "A Size-Dependent Shear Deformation Beam Model Based on the Strain Gradient Elasticity Theory," *International Journal of Engineering Science*,, **70**, pp. 1-14 (2013).
51. Nejad, M. Z., Hadi, A. and Rastgoo, A., "Buckling Analysis of Arbitrary Two-Directional Functionally Graded Euler–Bernoulli Nano-Beams Based on Nonlocal Elasticity Theory," *International Journal of Engineering Science*, **103**, pp. 1-10 (2016).
52. Romano, G. and Barretta, R., "Stress-Driven Versus Strain-Driven Nonlocal Integral Model for Elastic Nano-Beams," *Composites Part B: Engineering*, **114**, pp. 184-188 (2017).
53. Shishesaz, M., Hosseini, M., Naderan Tahan, K. and

https://doi.org/10.1017/jmech.2018.10 Published online by Cambridge University Press

Hadi, A., "Analysis of Functionally Graded Nano-disks under Thermoelastic Loading Based on the Strain Gradient Theory," *Acta Mechanica* (2017).

54. Romano, G., Barretta, R. and Diaco, M., "On Nonlocal Integral Models for Elastic Nano-Beams," *International Journal of Mechanical Sciences*, **131**, pp. 490-499 (2017).
55. Adeli, M. M., Hadi, A., Hosseini, M. and Gorgani, H. H., "Torsional Vibration of Nano-Cone Based on Nonlocal Strain Gradient Elasticity Theory," *The European Physical Journal Plus*, **132**, pp. 393 (2017).
56. Beni, Y. T., "A Nonlinear Electro-Mechanical Analysis of Nanobeams Based on the Size-Dependent Piezoelectricity Theory," *Journal of Mechanics*, **33**, pp. 289-301 (2016).
57. Hosseini, M., Gorgani, H. H., Shishesaz, M. and Hadi, A., "Size-Dependent Stress Analysis of Single-Wall Carbon Nanotube Based on Strain Gradient Theory," *International Journal of Applied Mechanics*, **9**, pp. 1750087 (2017).
58. Nejad, M. Z., Hadi, A. and Farajpour, A., "Consistent Couple-Stress Theory for Free Vibration Analysis of Euler-Bernoulli Nano-Beams Made of Arbitrary Bi-Directional Functionally Graded Materials," *Structural Engineering and Mechanics*, **63**, pp. 161-169 (2017).
59. Shishesaz, M., Zakipour, A. and Jafarzadeh, A., "Magneto-Elastic Analysis of an Annular FGM Plate Based on Classical Plate Theory Using GDQ Method," *Latin American Journal of Solids and Structures*, **13**, pp. 2736-2762 (2016).
60. Chen, Y. Z. and Lin, X. Y., "Elastic Analysis for Thick Cylinders and Spherical Pressure Vessels Made of Functionally Graded Materials," *Computational Materials Science*, **44**, pp. 581-587 (2008).

(Manuscript received July 7, 2017
accepted for publication February 8, 2018.)

https://doi.org/10.1017/jmech.2018.10 Published online by Cambridge University Press